Jurnal Polimesin
Department of Mechanical Engineering
State Polytechnic of Lhokseumawe
http://e-jurnal.pnl.ac.id/polimesin

e-ISSN	: 2549-1999	No.	: 1	Month	: February
p-ISSN	: 1693-5462	Volume	: 21	Year	: 2023

Received on 2022-09-03, Reviewed on 2022-10-07, Accepted on 2023-01-09, Copy edited on 2023-02-07, Layout edited on 2023-02-20 and Available online on 2023-02-28

The mixture of molybdate and ethoxylated fatty amines as corrosion protection in SAW weld joints of API 5L X-52 pipeline steel 3.5% NaCl solution: electrochemical study

Hery Tristijanto[1,a], Mochammad Noer Ilman[2,b], and Priyo Tri Iswanto[2,c]
[1]Department of Mechanical Engineering, State Polytechnic of Semarang, Semarang 50275, Indonesia
[2]Department of Mechanical and Industrial Engineering, University of Gadjah Mada, Yogjakarta 55281, Indonesia
Corresponding author:
[a]hery.tristijanto@mail.ugm.ac.id
[b]ilman_noer@ugm.ac.id and
[c]priyotri@ugm.ac.id

Abstract.

Steel widely used as pipelines in oil and gas transmission was susceptible to corrosion attack. In the present study, the corrosion inhibitions of Sodium Molybdate (SM) and Ethoxylated Fatty Amine (EFA) for corrosion of carbon steel (API 5L X-52 steel welded pipelines) at base metal (BM), weld metal (WM), and Heat Affected Zone (HAZ) in 3.5% NaCl solution was studied experimentally using potential dynamic polarization and Electrochemical Impedance Spectroscopy (EIS). The results indicated that Tafel polarization investigations showed that the corrosion potentials shift to a positive direction in the Based Metal (BM), HAZ, and Weld Metal (WM) areas, and the corrosion rate density moves to the left. The decreased corrosion rate was related to form a passive film on the steel surface. EIS measurements show that two-time constants appear, the first in the mid-high frequency range related to the corrosion process between the metal surface and Mo ions. The second in the low-frequency range is related to the formation of the two metal layers, Oxide/hydroxide. Thus, the corrosion protection of steel has been confirmed. The most excellent inhibitor efficiency, when the concentration of the SM was 0.4%, and EFA was 400 ppm, occurred in BM, WM, and HAZ, respectively.

Keywords:
Corrosions inhibition, potential dynamic polarization, tafel polarization, corrosions protections

1 Introduction

Carbon steels have been widely used as piping and pipeline materials in the oil and gas industry. Although their corrosion resistance was limited, these materials were preferred due to beneficial factors such as economy, availability, and high strength, as well as the fact that they are susceptible to corrosion attack [1], [2]. API 5L pipelines were used for transmission pipelines in the oil and gas industry and were made of ordinary carbon steel.

Carbon steels have been widely used as piping and pipeline materials in the oil and gas industry. Although their corrosion resistance was limited, these materials were preferred due to beneficial factors such as economy, availability, and high strength, as well as the fact that they are susceptible to corrosion attack [1], [2]. API 5L pipelines are used for transmission pipelines in the oil and gas industry, and they are made of ordinary carbon steel.

Various methods have been used to control corrosion, such as cathodic protection, coatings, inhibitors, etc. Among these corrosion protection methods, the corrosion inhibitor seems to be beneficial because a small amount of inhibitor added to the corrosive solution is sufficient to reduce the corrosion rate or prevent it. Corrosion inhibitors are classified into organic and inorganic. Several studies on corrosion inhibitors have been conducted, including molybdenum-organic inhibitors in sodium chloride solutions for corrosion protection of carbon steel, such as molybdate, tungstate, and nitrite ions on carbon steel [3], nitrite and molybdate anions on mild steel [4][5], sodium molybdate and 1H-Benzotriazole on mild steel [6][7], blends of molybdate, nitrite, and picrate on mild steel [8], etc. Research on corrosion inhibitors using amine derivatives in carbon steel is shown in Table 1. Inhibitor performance is difficult to predict without carrying out comprehensive experimental work. Some common methods that have been used to analyse the corrosion rate was electrochemical impedance spectroscopy [9], electrochemical polarization [10], and weight loss [11].

Table 1. Research on the use of amine-based corrosion inhibitors

Material	Inhibitor	Media	Ref.
Mild steel	Quaternary ammonium, amide, and amine	1 M HCl	[12]
Carbon steel	3,3-diamino dipropyl amine	2 N HCl	[13]
Carbon steel	Ethoxylated pentamine oleamide	1 M HCl	[14]
Pipeline steel	N-(5-nitro-2-hydroxybenzylidene) pyridine-4-amine	1 M HCl	[15]
Mild steel	Epoxidized soybean fatty acids/ρ-substituted aromatic amines	UV irradiation	[16]
X-80	3-Methoxypropyl-amine	Simulated saline water	[17]
Carbon steel	Methionine	Carbon capture	[18]
Carbon steel	N,N′-di-β-D-glucopyranosylethylenediamine, N-benzyl-N,N-bis[(3,5-dimethyl-1H-pyrazol-1-yl) methyl]amine	Molasses	[19]
Stainless steel	Amine grafted poly-(acrylic maleic)	3.5 % NaCl	[20]
Carbon steel	Amine 4-amino-1-propyl-piperidine	Aquades, CO_2	[21]
X-80	3-(2-chloro-5,6-dihydrobenzo[b][1] benzazepin-11-yl)-N, N- dimethylpropan-1-amine	HCl	[22]
Carbon steel	Hexamethylene tetramine	HCl	[23]
Mild steel	(Z)-N-(2-chlorobenzylidene) naphthalen-1-amine dan (Z)-N-(3-nitrobenzylidene) naphthalen-1- amine	HCl	[24]

Although there have been extensive studies on the inhibitory effect of molybdate-organic inhibitors and amines-based on carbon steel, especially in the X-52 steel pipe, research on the synergy between molybdate and ethoxylated fatty amine on carbon steel in 3.5% NaCl environment has not been carried out. This paper is aimed to investigate the electrochemical corrosion behaviour of carbon steel in a 3.5% NaCl solution with a mixture of SM and EFA as a corrosion inhibitor.

2 Experimental method

2.1 Material

Specimens having a diameter of 15 mm and thickness of 4 mm were taken from the BM, HAZ, and WM of carbon steel (API 5L X-52 steel pipelines). The chemical compositions of the steel pipelines are shown in Table 2. Specimens were polished up to 2000 grade with abrasive paper manually until the surface was like glass, rinsed with deionized water, and decreased in 96% ethanol.

Table 2. API 5L X-52 steel pipelines and filler metal chemical compositions, (wt. %) [25]

Element	C	Mn	Si	S	Cu	Ni	Cr	Mo	Ti	Al	Nb
Base	0.06	1.141	0.19	0.00	0.00	0.00	0.02	0.002	0.01	0.03	0.04
Weld	0.07	0.253	0.33	0.00	0.02	0.01	0.02	0.003	0.00	0.02	0.02

Filler	0.09	1.12	0.20	0.00	0.06

2.2 Corrosion solutions and inhibitors

The corrosion solution was 3.5% NaCl which was dissolved in distilled water as a basic solution. The mixture of corrosion inhibitors concentration, sodium molybdate (SM), and ethoxylated fatty amine (EFA) in the basic solution was 0.1% SM + 100 ppm EFA, 0.2% SM + 200 ppm EFA, 0.3% SM + 300 ppm EFA, and 0.4% SM + 400 ppm EFA. The chemical structure of EFA was presented in Fig. 1.

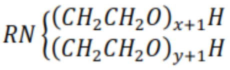

$$RN\begin{cases}(CH_2CH_2O)_{x+1}H\\(CH_2CH_2O)_{y+1}H\end{cases}$$

Fig. 1. Ethoxylated fatty amine chemical structure [26]

2.3 Electrochemical measurement

Electrochemical measurements were made using the VersaSTAT 4.0 potentiostat, VersaStudio, and the results were analysed using the ZSimpWin software package provided by Princeton Applied Research, United States. Two graphite bars and a saturated calomel electrode (SCE) were used as the auxiliary and the reference electrodes, respectively. The working electrodes were prepared from the X-52 steel pipelines.

The Tafel polarization is set at -2.4 to 2.4 mV with a scan rate of 1 mVs^{-1}. EIS was set at a voltage amplitude of 10 mV with 8 points per decade and a frequency range of 0.01 to 100 kHz.

3 Result and discussion

3.1 Tafel polarization measurement

The Tafel polarization diagrams of the X-52 steel pipe weld joint in a 3.5% NaCl solution without and with different inhibitor concentrations were shown in Fig. 2. Generally, the Tafel plots in the BM, HAZ and WM regions show that the potential corrosion moved in a positive direction. The corrosion current density was reduced less than that without inhibitors. Increasing the concentration of inhibitor compounds causes a decrease in the corrosion rate, which was indicated by the decreasing current density to the left. This illustrates the formation of a passive layer on the surface of X-52 steel [27].

Tafel polarization parameters such as corrosion potential (E_{cor}), corrosion current density (I_{cor}), cathode slope (βc), and anode (βa) Tafel were given in Table 3. The cathodic branch represents the hydrogen evolution reaction, whereas the anodic branch represents the iron dissolving reaction under experimental conditions [12]. Changes in the cathodic (βc) and anodic (βa) Tafel slopes with increasing inhibitor concentrations indicate that SM and EFA changed the oxygen and hydrogen reduction reactions or iron dissolution mechanism occurred [28]. The difference between β_c and β_a at HAZ was slightly higher, and this difference indicates that this inhibitor controls both [14]. The anodic slope increased with increasing concentration of molybdate in the solution inhibitor added. However, it should be noted that this parameter was also influenced by the inhibitor film formed [29][30].

The corrosion potentials in the BM, from -572.817 to -464.160 mV, and WM, from -621.563 to -454.148 mV regions were more positive at each concentration of the two inhibitors compared to the corrosion potential in the HAZ, from -638.447 to -525.371 mV. This shows that in a 3.5% NaCl solution containing SM and EFA, BM has the ability to act as a cathode relative to HAZ [31].

3.2 EIS Measurement

The Nyquist and Bode diagram for API 5L X-52 steel pipe in 3.5% NaCl solution without and with corrosion-inhibiting compounds with different concentrations (Fig. 3). Table 3 shows the parameters of the EIS results in this test. EIS results in Table 2 show that the charge transfer resistance value (R_{ct}) increases with increasing inhibitor concentration; this may indicate that a protective layer was formed on the steel surface. This layer provides a barrier for mass and charge transfer [16].

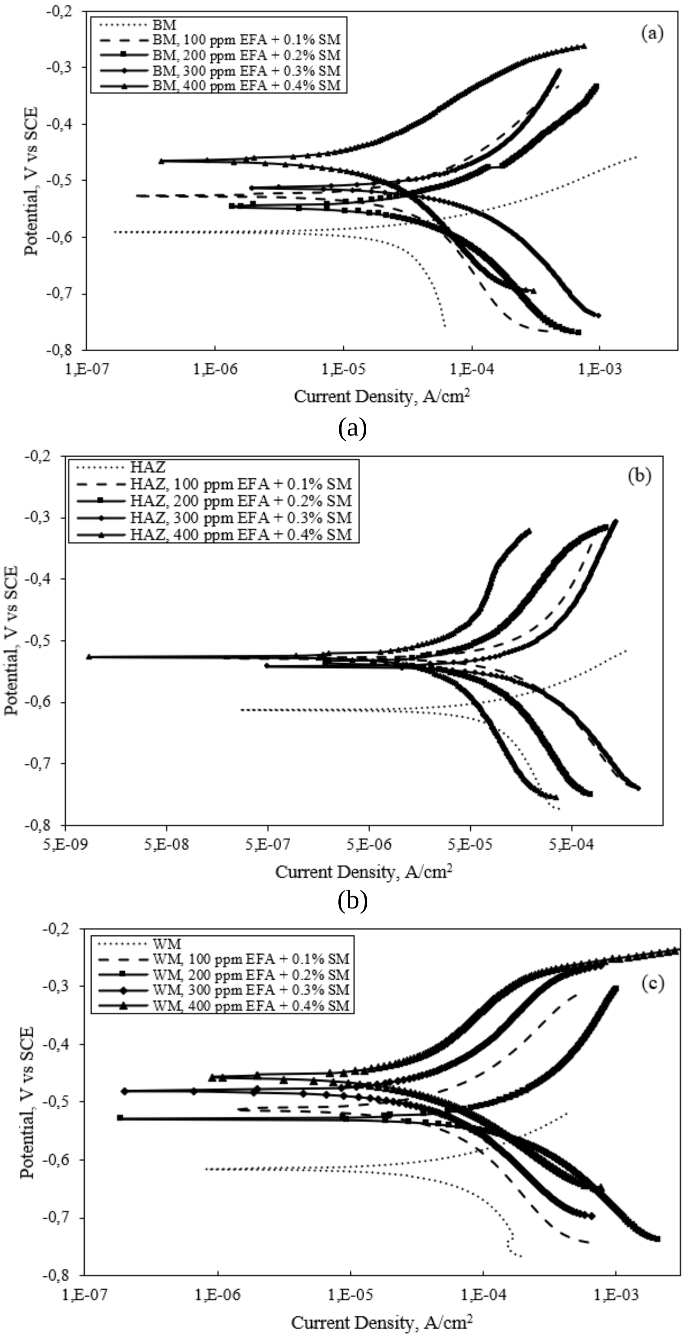

(a)

(b)

(c)

Fig. 2. Tafel polarization curve of X-52 steel in the area of base Metal. (a) HAZ, (b) WB, and (c) in 3.5% NaCl absence and presence corrosion inhibiting compounds (SM and EFA) with different concentrations

The R_{ct} value is the resistance between the metal and the Helmholtz Outer Plane (OHP). The decrease in double-layer capacitance, C_{dl}, can be caused by a decrease in the local dielectric constant and an increase in the thickness of the electric double layer; this indicates that the corrosion inhibitor compound molecules function by adsorption at the metal/solution interface [14]. The inhibition efficiency was calculated from EIS measurement with eq. (1).

$$IE\% = \left(1 - \frac{R_f}{R_{ct}}\right) \qquad (1)$$

where R_f and R_{ct} are the charge transfer resistance in the absence and presence of the inhibitor, respectively, based on Table 4, the highest inhibitor efficiency was achieved when the concentration of the SM was 0.4%, and EFA was 400ppm, and this occurred in BM, WM and HAZ.

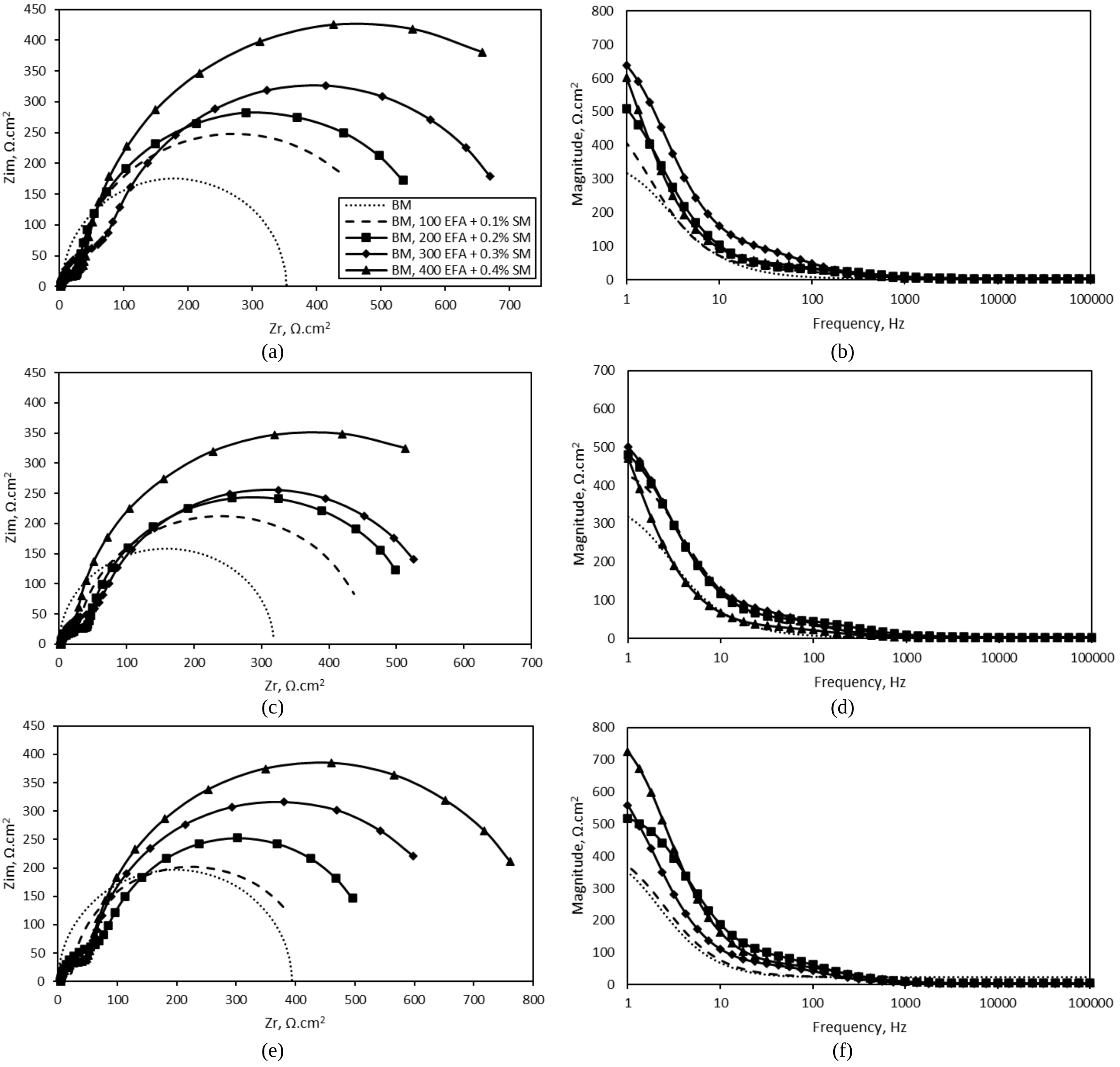

Fig. 3. (a, c, d) Nyquist and Bode and (b, d, f) diagrams for X-52 pipeline steel in 3.5% NaCl absence and present corrosion inhibitor compounds with different concentration

Table 3. Tafel polarization parameters of steel X-52 in the BM, HAZ, and WM regions in 3.5% NaCl at different concentrations of SM and EFA

Regions	Na_2MoO_4 (%)	EFA (ppm)	$V_{cor,}$ (mV_{SCE})	CR (mmpy)	I_{cor} ($\mu A/cm^2$)	β_c (mV/dec)	β_a (mV/dec)
Base Metal	0	0	-572.817	0.298	51.713	185.984	63.314
	0.1	100	-526.287	0.173	26.476	118.430	118.430
	0.2	200	-546.803	0.324	46.738	148.000	148.000
	0.3	300	-513.511	0.499	77.275	181.788	181.788
	0.4	400	-464.160	0.067	10.330	115.938	115.938
HAZ	0	0	-638.447	0.722	125.170	175.774	80.222
	0.1	100	-864.108	0.673	97.104	186.713	186.713
	0.2	200	-534.632	0.249	38.672	118.365	118.365
	0.3	300	-538.234	0.748	134.472	122.395	122.395
	0.4	400	-525.371	0.079	12.051	90.227	90.227
Weld Metal	0	0	-621.563	0.364	63.078	162.973	73.813
	0.1	100	-515.006	0.186	26.787	98.269	98.269
	0.2	200	-529.238	0.569	88.228	117.607	117.607
	0.3	300	-480.484	0.124	19.185	99.195	99.195
	0.4	400	-454.148	0.102	15.832	100.025	100.025

Magnitude in the Bode diagram of API 5L X-52 steel in 3.5% NaCl solution without and with corrosion inhibitor compound shows an increase in the impedance magnitude at low frequencies, as shown in Figures 3b, d, and f. This confirms that the higher the inhibitor concentration, the higher the corrosion protection on the steel surface [33].

Considering the Nyquist and Bode plots in Fig. 3 for the corrosion inhibitors SM and EFA, two-time constants appear. One in the medium-high frequency range is related to the corrosion process as well as the Mo-rich film layer between the steel surface and the Mo ions. The second in the low-frequency range is associated with the formation of the second metal oxide/hydroxide layer [34] or corresponds to the charge transfer process that occurs on the steel surface [35]. Table 4, the R_{ct} value increased significantly after the addition of inhibitors at BM from 644.7 to 982.6 $\Omega.cm^2$; at HAZ from 414.0 to 813.1 $\Omega.cm^2$; at WM from 639.0 to 692.5 $\Omega.cm^2$; which reflects that all inhibitors have an inhibitory effect on the carbon steel surface. The values of electric double layer capacitors (C_{dl}) and film capacitors (C_f) show a decreasing trend at BM from 1.58E-4 to 1.47E-4 F.cm^2; at WM from 1.32E-4 to 1.04E-4 F.cm^2; except at HAZ from 1.19E-4 to 1.86E-4; which was due to the fact that the dielectric constant of corrosion inhibitors was smaller than that of water and the absorption of inhibitors increased in width. The electrical double coating on the surface of the steel results in a significant reduction in capacitance [35].

Table 4. EIS results of X-52 steel in the area of BM, HAZ, and WM in 3.5% NaCl without and with corrosion-inhibiting compounds (SM and EFA) with different concentrations

Region	Na_2MoO_4 (%)	EFA (ppm)	R_s (Ωcm^2)	C_f (Fcm^2)	R_f (Ωcm^2)	C_{dl} (Fcm^2)	R_{ct} (Ωcm^2)	IE (%)
BM	0	0	4.189	2.23E-04	349.400	-	-	-
	0.1	100	4.124	3.74E-05	44.620	1.58E-04	644.7	87.9
	0.2	200	2.079	2.62E-05	26.910	1.90E-04	445.8	89.5
	0.3	300	1.720	5.50E-05	63.590	2.04E-04	325.5	90.3
	0.4	400	2.903	2.99E-05	63.160	1.47E-04	982.6	93.0
HAZ	0	0	0.179	2.68E-05	318.000	-	-	
	0.1	100	3.139	1.98E-05	35.520	1.19E-04	414.0	85.9
	0.2	200	2.888	1.77E-05	51.630	1.43E-04	477.0	87.7
	0.3	300	2.311	3.32E-05	63.770	1.93E-04	172.4	87.6
	0.4	400	2.581	4.45E-05	40.870	1.86E-04	813.1	91.5
WM	0	0	0.099	2.63E-04	392.800	-	-	
	0.1	100	2.299	1.50E-05	43.500	1.32E-04	639.0	90.8
	0.2	200	2.378	5.01E-05	44.500	2.25E-04	184.6	86.9
	0.3	300	2.665	3.42E-05	58.530	1.93E-04	507.2	90.4
	0.4	400	4.859	1.86E-05	62.210	1.04E-04	692.5	92.2

4 Conclusions

1. In general, in the BM, HAZ, and WM areas, the corrosion potentials shift to a positive direction, and the corrosion rate density moves to the left so that the mixed compound between sodium molybdate and the ethoxylated fatty amine was predicted to be an anodic inhibitor.
2. Two-time constants appear, the first in the medium-high frequency range associated with the corrosion process between the metal surface and Mo ions and the second in the low-frequency range, which was related to the formation of both metal oxide/hydroxide layers.
3. The most excellent inhibitor efficiency when the concentration of the SM was 0.4% and EFA was 400 ppm occurred in BM, WM, and HAZ, respectively

References

[1] A. H. Tantawy, K. A. Soliman, and H. M. Abd El-Lateef, “Novel synthesized cationic surfactants based on natural piper nigrum as sustainable-green inhibitors for steel pipeline corrosion in CO2-3.5%NaCl: DFT, Monte Carlo simulations and experimental approaches,” *J Clean Prod*, vol. 250, p. 119510, 2020, doi: 10.1016/j.jclepro.2019.119510.

[2] M. Heydari and M. Javidi, “Corrosion inhibition and adsorption behaviour of an amido-imidazoline derivative on API 5L X52 steel in CO 2-saturated solution and synergistic effect of iodide ions,” *Corros Sci*, vol. 61, pp. 148–155, 2012, doi: 10.1016/j.corsci.2012.04.034.

[3] M. A. Deyab and S. S. A. El-rehim, “Inhibitory effect of tungstate, molybdate and nitrite ions on the carbon steel pitting corrosion in alkaline formation water containing Cl − ion,” *Electrochim Acta*, vol. 53, pp. 1754–1760, 2007, doi: 10.1016/j.electacta.2007.08.024.

[4] Y. Zhou and Y. Zuo, “The inhibitive mechanisms of nitrite and molybdate anions on initiation and propagation of pitting corrosion for mild steel in chloride solution,” *Appl Surf Sci*, vol. 353, no. 2, pp. 924–932, 2015, doi: 10.1016/j.apsusc.2015.07.037.

[5] A. A. Al-Refaie, J. Walton, R. A. Cottis, and R. Lindsay, “Photoelectron spectroscopy study of the inhibition of mild steel corrosion by molybdate and nitrite anions,” *Corros Sci*, vol. 52, no. 2, pp. 422–428, 2010, doi: 10.1016/j.corsci.2009.09.030.

[6] K. S. Bokati, C. Dehghanian, and M. Babaei, “Influence of Near-Surface Severe Plastic Deformation of Mild Steel on the Inhibition Performance of Sodium Molybdate and 1H-Benzotriazole in Artificial Sea Water,” *J Mater Eng Perform*, vol. 27, no. 2, pp. 550–559, 2018, doi: 10.1007/s11665-018-3130-3.

[7] K. Sabet Bokati, C. Dehghanian, and S. Yari, “Corrosion inhibition of copper, mild steel and galvanically coupled copper-mild steel in artificial sea water in presence of 1H-benzotriazole, sodium molybdate and sodium phosphate,” *Corros Sci*, vol. 126, no. July, pp. 272–285, 2017, doi: 10.1016/j.corsci.2017.07.009.

[8] F. B. Ravari, S. Mohammadi, and A. Dadgarinezhad, “Corrosion inhibition of mild steel in stimulated cooling water by blends of molybdate, nitrite and picrate as new anodic inhibitor,” *Anti-Corrosion Methods and Materials*, vol. 59, no. 4, pp. 182–189, 2012, doi: 10.1108/00035591211242014.

[9] P. Li, J. Y. L. K. L. Tanb, and J. Y. Leea, “Electrochemical impedance and X-ray photoelectron spectroscopic studies of the inhibition of mild steel corrosion in acids by cyclohexylamine,” vol. 42, no. 4, pp. 605–615, 1997.

[10] J. M. Æ. R. Duran-romero, “Electrochemical evaluation of aminotriazole corrosion inhibitor under flow conditions,” *Journal* Application *ElectrochemA*, vol. 39, pp. 1809–1819, 2009, doi: 10.1007/s10800-009-9884-4.

[11] M. Sharma, A. V. R. Kumar, and N. Singh, “Electrochemical Evaluation Of The Synergistic Effect Of Molybdate Tungstate Inhibitor Mixtures In Chloride Ion Medium And Effect Of Cl - Ion On Inhibition Efficiency Of Molybdate,” vol. 61, no. June, pp. 251–254, 2008, doi: 10.1007/s12666-008-0030-5.

[12] D. S. Chauhan, M. A. Quraishi, M. A. Jafar Mazumder, S. A. Ali, N. A. Aljeaban, and B. G. Alharbi, “Design and synthesis of a novel corrosion inhibitor embedded with quaternary ammonium, amide and amine motifs for protection of carbon steel in 1 M HCl,” *J Mol Liq*, vol. 317, Nov. 2020, doi: 10.1016/j.molliq.2020.113917.

[13] H. Kumar and M. Kumari, “Experimental and theoretical investigation of 3,3′-diamino dipropyl amine: Highly efficient corrosion inhibitor for carbon steel in 2 N HCl at normal and elevated temperatures,” *J Mol Struct*, vol. 1229, Apr. 2021, doi: 10.1016/j.molstruc.2020.129598.

[14] M. R. Mishrif, M. R. Noor El-Din, and E. A. Khamis, “Utilization of ethoxylated pentamine oleamide as new Gemini surfactants for corrosion inhibition effectiveness in 1 M HCl solution,” *Egyptian Journal of Petroleum*, vol. 27, no. 4, pp. 1357–1370, Dec. 2018, doi: 10.1016/j.ejpe.2018.09.004.

[15] N. B. Iroha, C. U. Dueke-Eze, A. O. James, and T. M. Fasina, “Newly synthesized N-(5-nitro-2-hydroxybenzylidene)pyridine-4-amine as a high-potential inhibitor for pipeline steel corrosion in hydrochloric acid medium,” *Egyptian Journal of Petroleum*, vol. 30, no. 2, pp. 55–61, Jun. 2021, doi: 10.1016/j.ejpe.2021.02.003.

[16] I. M. Mousaa, “Gamma irradiation processed (epoxidized soybean fatty acids/ρ-substituted aromatic amines) adducts as corrosion inhibitors for UV–curable steel coatings,” *Prog Org Coat*, vol. 111, pp. 220–230, Oct. 2017, doi: 10.1016/j.porgcoat.2017.06.009.

[17] K. H. Rashid and A. A. Khadom, “3-Methoxypropyl-amine as corrosion inhibitor for X80 steel in simulated saline water,” *J Mol Liq*, vol. 319, Dec. 2020, doi: 10.1016/j.molliq.2020.114326.

[18] B. Udayappan and A. Veawab, “Performance analysis of methionine as an environmentally friendly corrosion inhibitor for carbon steel in the amine based carbon capture process,” *International Journal of Greenhouse Gas Control*, vol. 114, Feb. 2022, doi: 10.1016/j.ijggc.2021.103565.

[19] A. Cherubin, J. Guerra, E. Barrado, C. García-Serrada, and F. J. Pulido, “Addition of amines to molasses and lees as corrosion inhibitors in sustainable de-icing materials,” *Sustain Chem Pharm*, vol. 29, Oct. 2022, doi: 10.1016/j.scp.2022.100789.

[20] T. A. Saleh, K. Haruna, M. M. Nur, and B. Alharbi, “Synthesis of Amine Grafted Poly (Acrylic-Maleic) as an efficient inhibitor against stainless steel corrosion in a highly saline medium,” *Prog Org Coat*, vol. 170, Sep. 2022, doi: 10.1016/j.porgcoat.2022.106974.

[21] X. Li, P. Pearson, Q. Yang, G. Puxty, P. Feron, and D. Xiao, “A study of designer amine 4-amino-1-propyl-piperidine against the corrosion of carbon steel for application in CO2 capture,” *International Journal of Greenhouse Gas Control*, vol. 94, Mar. 2020, doi: 10.1016/j.ijggc.2019.102929.

[22] E. B. Ituen and J. E. Asuquo, “Inhibition of X80 steel corrosion in oilfield acidizing environment using 3-(2-chloro-5,6-dihydrobenzo[b][1]benzazepin-11-yl)-N,N-dimethylpropan-1-amine and its blends,” *J King Saud Univ Sci*, vol. 31, no. 1, pp. 127–135, Jan. 2019, doi: 10.1016/j.jksus.2017.06.009.

[23] J. Biswal, H. J. Pant, S. C. Sharma, and A. K. Gupta, “Investigation of effect of an amine inhibitor on corrosion of carbon steel by using thin layer activation technique,” *J Radioanal Nucl Chem*, vol. 323, no. 3, pp. 1339–1345, Mar. 2020, doi: 10.1007/s10967-019-06710-7.

[24] E. E. Elemike, H. U. Nwankwo, and D. C. Onwudiwe, “Experimental and theoretical studies of (Z)-N-(2-chlorobenzylidene) naphthalen-1-amine and (Z)-N-(3-nitrobenzylidene) naphthalen-1-amine, and their corrosion inhibition properties,” *J Mol Struct*, vol. 1155, pp. 123–132, Mar. 2018, doi: 10.1016/j.molstruc.2017.10.102.

[25] H. Tristijanto, M. N. Ilman, and P. Tri Iswanto, “Corrosion Inhibition of Welded of X – 52 Steel Pipelines by Sodium Molybdate in 3.5% NaCl Solution,” *Egyptian Journal of Petroleum*, vol. 29, no. 2, pp. 155–162, Jun. 2020, doi: 10.1016/j.ejpe.2020.02.001.

[26] L. Hamadi, S. Mansouri, K. Oulmi, and A. Kareche, “The use of amino acids as corrosion inhibitors for metals: A review,” *Egyptian* Journal *of Petroleum*, vol. 27, no. 4. Egyptian Petroleum Research Institute, pp. 1157–1165, Dec. 01, 2018. doi: 10.1016/j.ejpe.2018.04.004.

[27] Q. Qu, L. Li, S. Jiang, W. Bai, and Z. Ding, “Effect of sodium molybdate on the corrosion behavior of cold rolled steel in peracetic acid solution,” *J Appl Electrochem*, vol. 39, no. 5, pp. 569–576, 2009, doi: 10.1007/s10800-008-9694-0.

[28] M. Mobin, M. Parveen, and M. Z. A. Rafiquee, “Synergistic effect of sodium dodecyl sulfate and cetyltrimethyl ammonium bromide on the corrosion inhibition behavior of L-methionine on mild steel in acidic medium,” *Arabian Journal of Chemistry*, vol. 10, pp. S1364–S1372, Feb. 2017, doi: 10.1016/j.arabjc.2013.04.006.

[29] M. A. Osipenko, D. S. Kharytonau, A. A. Kasach, J. Ryl, J. Adamiec, and I. I. Kurilo, “Inhibitive effect of sodium molybdate on corrosion of AZ31 magnesium alloy in chloride solutions,” *Electrochim Acta*, vol. 414, May 2022, doi: 10.1016/j.electacta.2022.140175.

[30] S. Chen, S. chun Wang, Y. Suo, G. Yang, Y. Du, and Y. Ren, “Inhibition effect of tannic acid and sodium molybdate for the flow corrosion of 304 stainless steel on 90° elbow,” *Journal of Materials Research and Technology*, vol. 20, pp. 2408–2420, Sep. 2022, doi: 10.1016/j.jmrt.2022.07.191.

[31] L. W. Wang, Z. Y. Liu, Z. Y. Cui, C. W. Du, X. H. Wang, and X. G. Li, “In situ corrosion characterization of simulated weld heat affected zone on API X80 pipeline steel,” *Corros Sci*, vol. 85, pp. 401–410, 2014, doi: 10.1016/j.corsci.2014.04.053.

[32] R. Farahmand, B. Sohrabi, A. Ghaffarinejad, and M. R. Zamani Meymian, “Synergistic effect of molybdenum coating and SDS surfactant on corrosion inhibition of mild steel in presence of 3.5% NaCl,” *Corros Sci*, vol. 136, no. April 2017, pp. 393–401, 2018, doi: 10.1016/j.corsci.2018.03.030.

[33] M. Mobin and R. Aslam, “Experimental and theoretical study on corrosion inhibition performance of environmentally benign non-ionic surfactants for mild steel in 3.5 % NaCl solution,” *Process Safety and Environmental Protection*, vol. 114, pp. 279–295, 2013, doi: 10.1016/j.psep.2018.01.001.

[34] I. A. Kartsonakis, S. G. Stanciu, A. A. Matei, R. Hristu, A. Karantonis, and C. A. Charitidis, “A comparative study of corrosion inhibitors on hot-dip galvanized steel,” *Corros Sci*, vol. 112, pp. 289–307, 2016, doi: 10.1016/j.corsci.2016.07.030.

[35] J. Shi, M. Wu, and J. Ming, “In-depth insight into the role of molybdate in corrosion resistance of reinforcing steel in chloride-contaminated mortars,” *Cem Concr Compos*, vol. 132, Sep. 2022, doi: 10.1016/j.cemconcomp.2022.104628.

Click or tap here to enter text.